Table of Contents

Phenotypes	$FH^{R/R}$ + control Ab		$FH^{R/R}$ + anti-P Ab once-weekly		$FH^{R/R}$ + anti-P Ab twice-weekly	
	Incidence (%)					
Neurological abnormalities	7/15	(46.7)	0/10	(0)	0/5	(0)
Brain thrombi	2/15	(13.3)	0/10	(0)	0/5	(0)
Brain ischemic change	5/15	(33.3)	0/10	(0)	0/5	(0)
Lung thrombi	1/15	(6.7)	0/10	(0)	0/5	(0)
Heart thrombi	0/15	(0)	0/10	(0)	0/5	(0)
Liver thrombi	11/15	(73.3)	1/10	(10.0)	1/5	(20.0)
Spleen thrombi	5/15	(33.3)	0/10	(0)	0/5	(0)

($FH^{R/R}$ + control Ab n = 15, $FH^{R/R}$ + anti-P once weekly n = 10, $FH^{R/R}$ + anti-P twice-weekly n = 5)

Supplemental Table 1

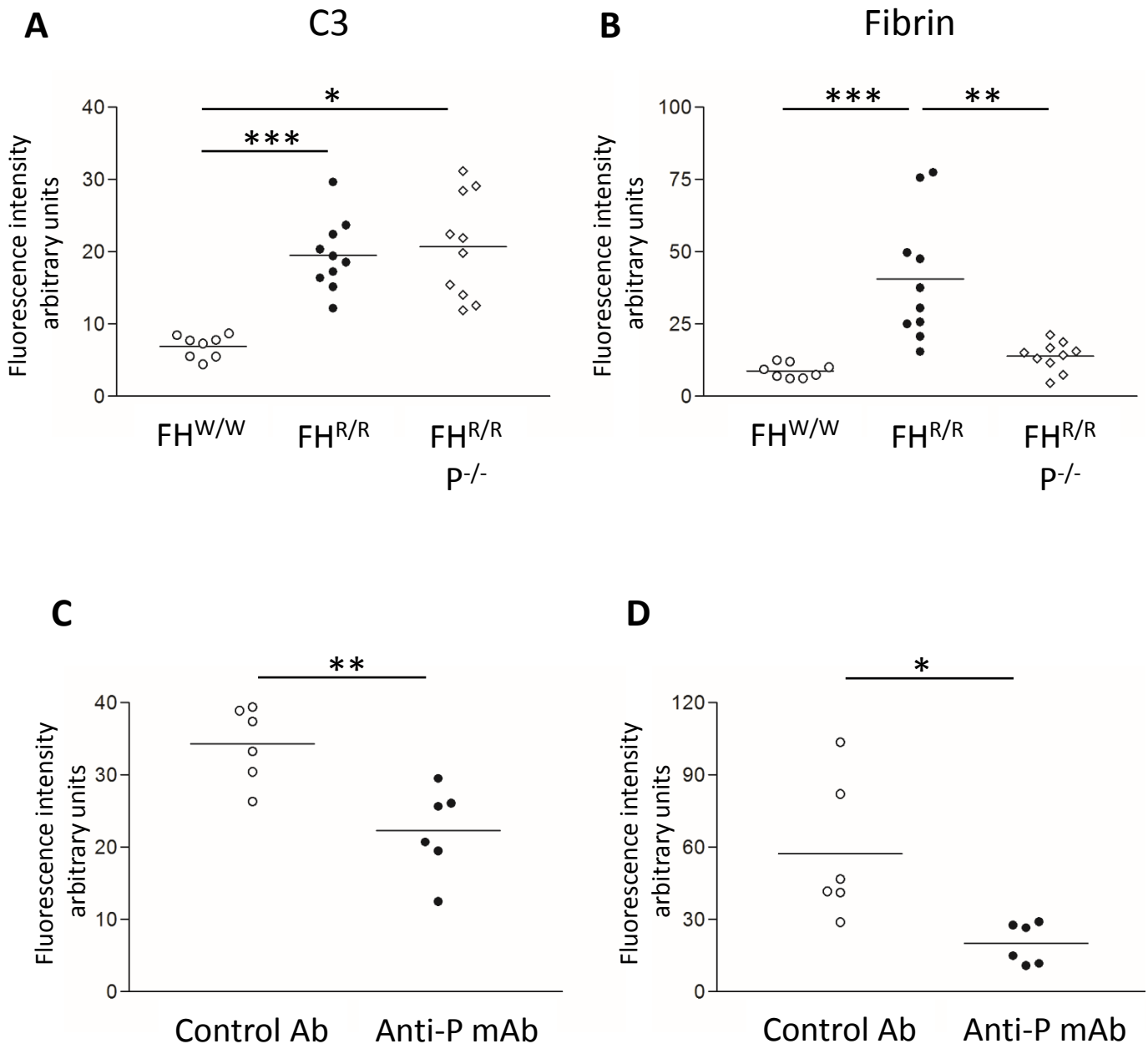

Supplemental Figure 1.

A

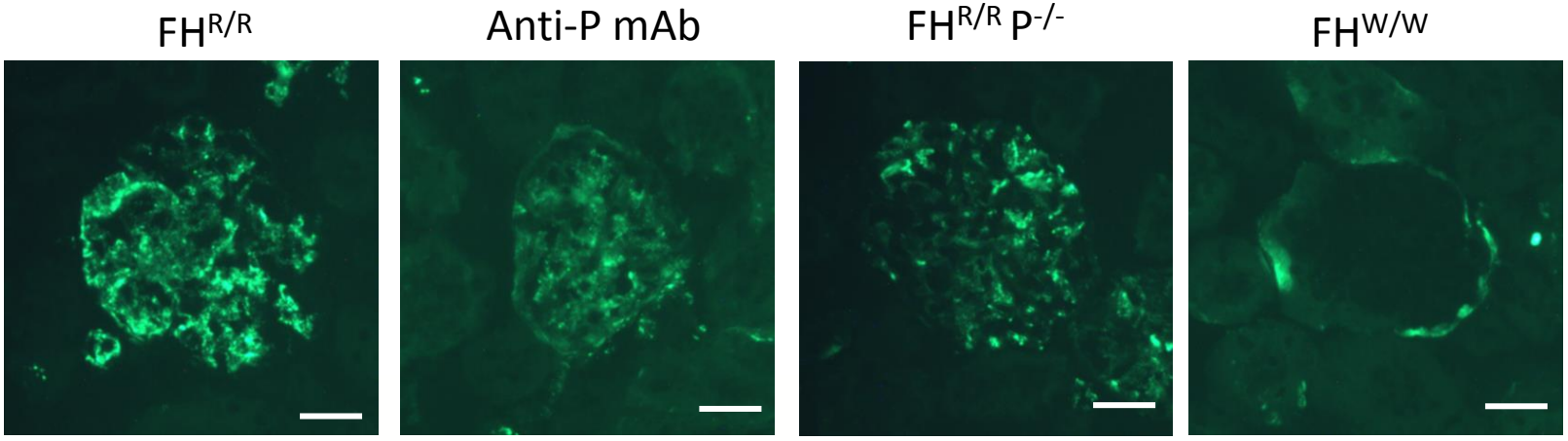

Scale bars = 25μm

B

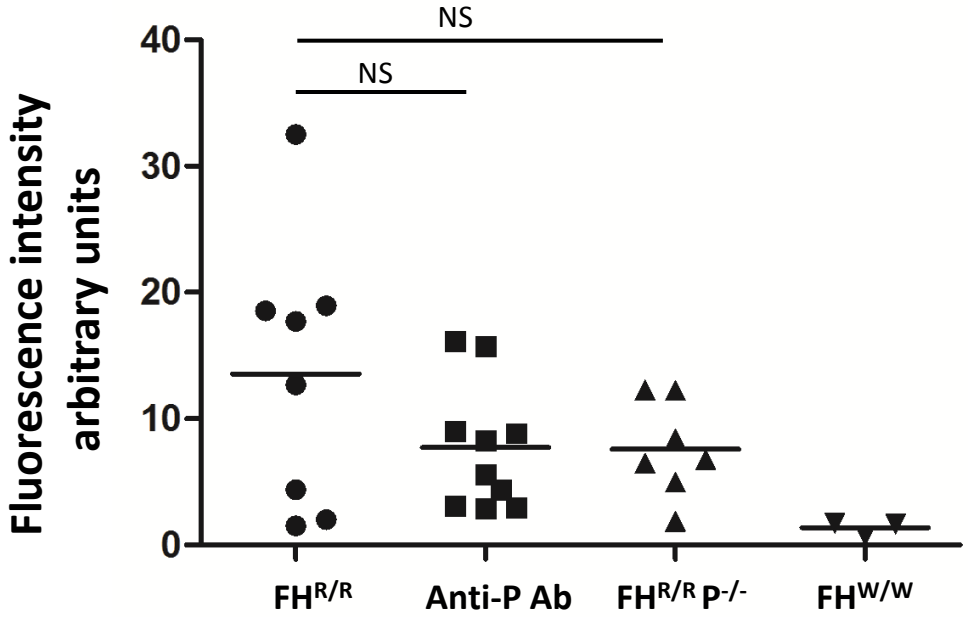

Supplemental Figure 2.

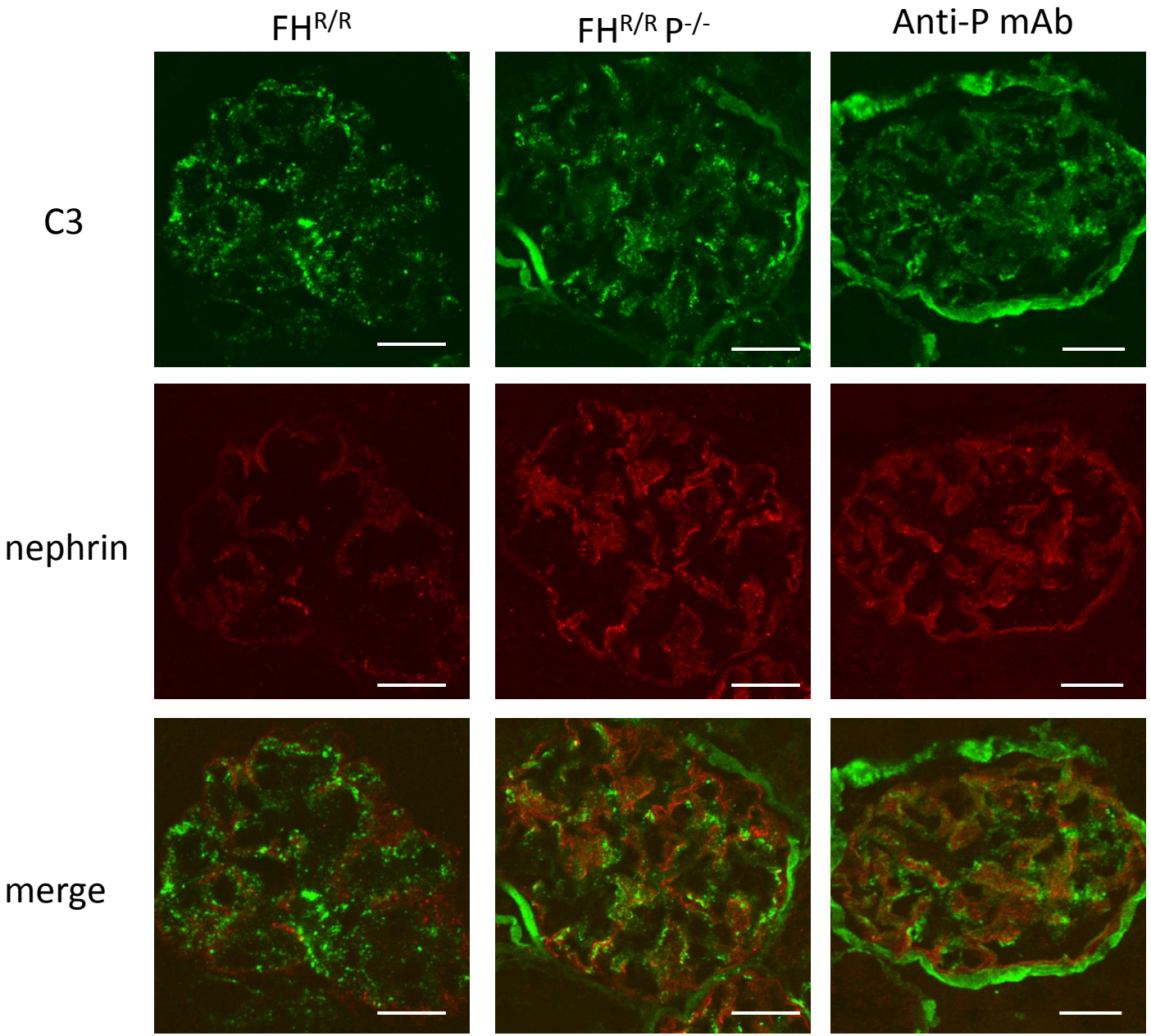

Supplemental Figure 3.

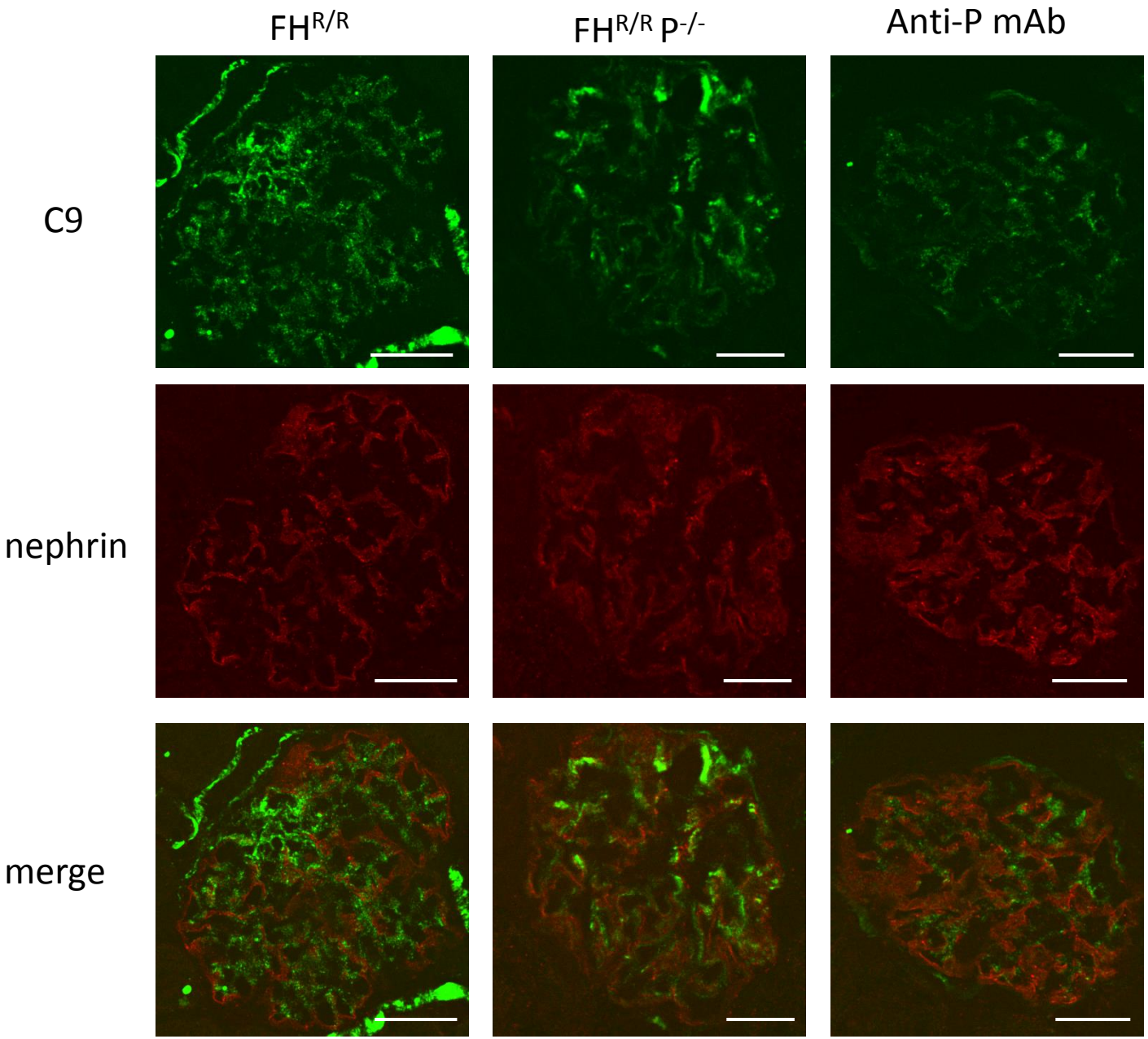

Supplemental Figure 4.

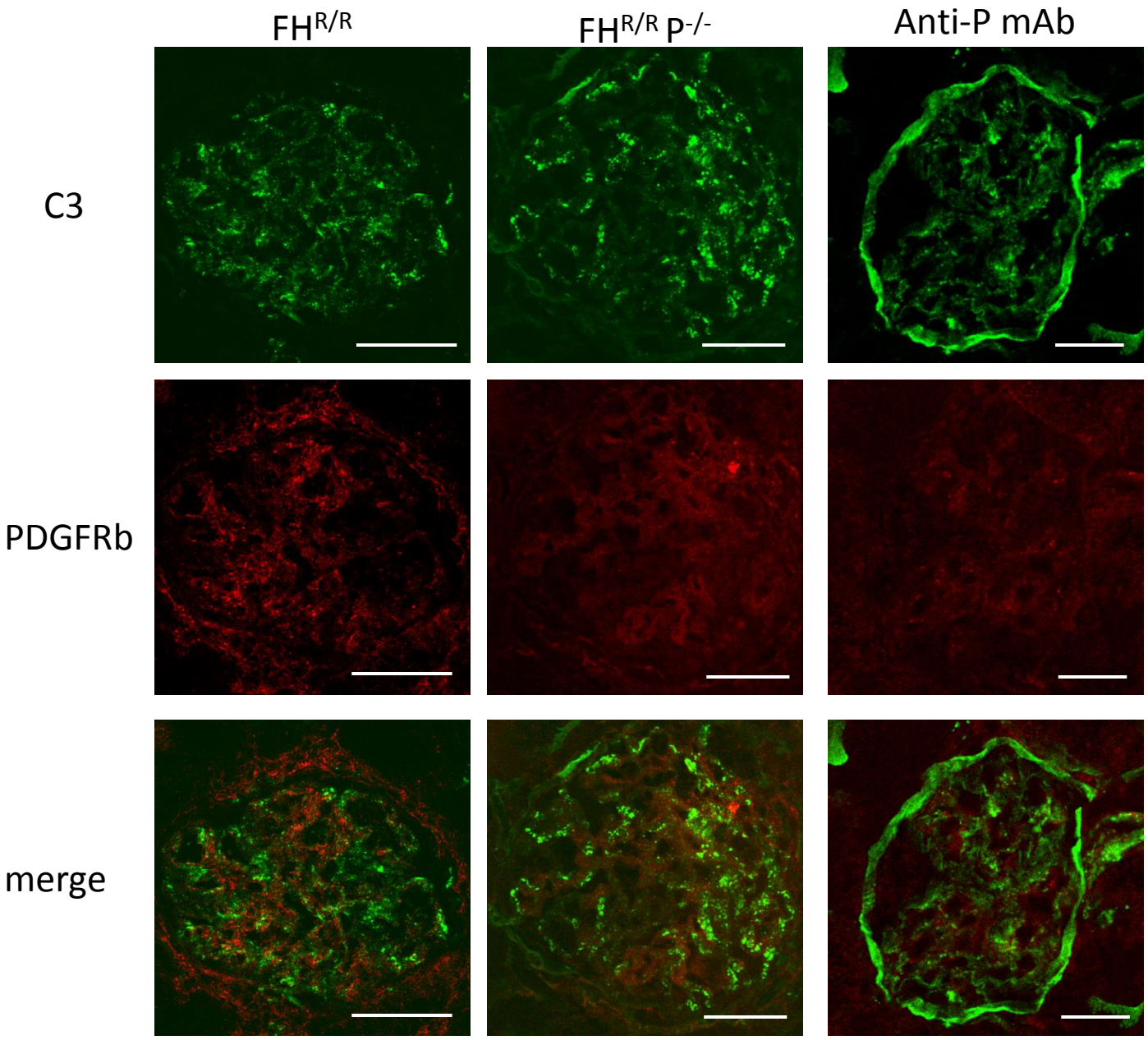

Supplemental Figure 5.

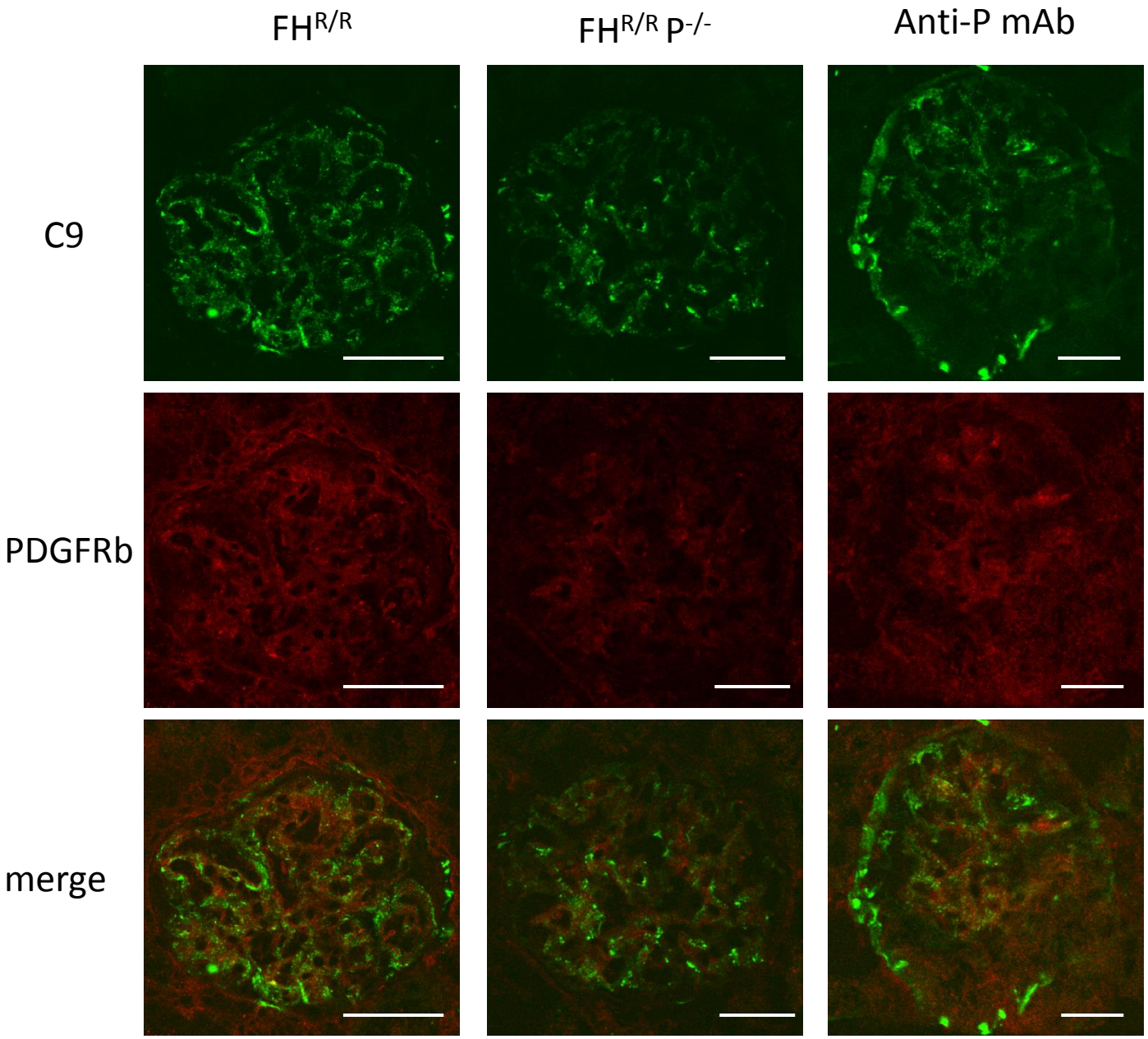

Scale bars=15μm

Supplemental Figure 6.

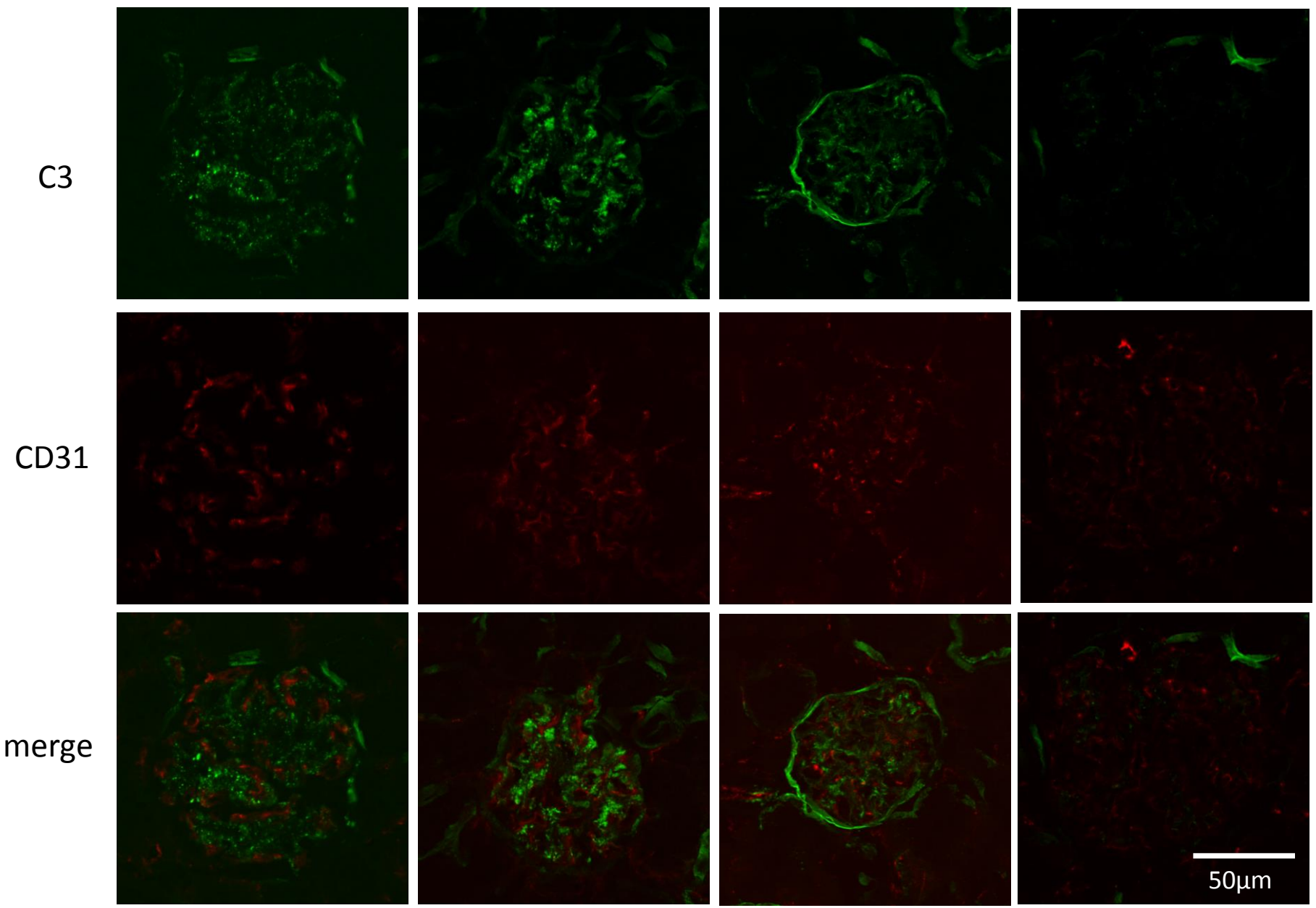

Supplemental Figure 7.

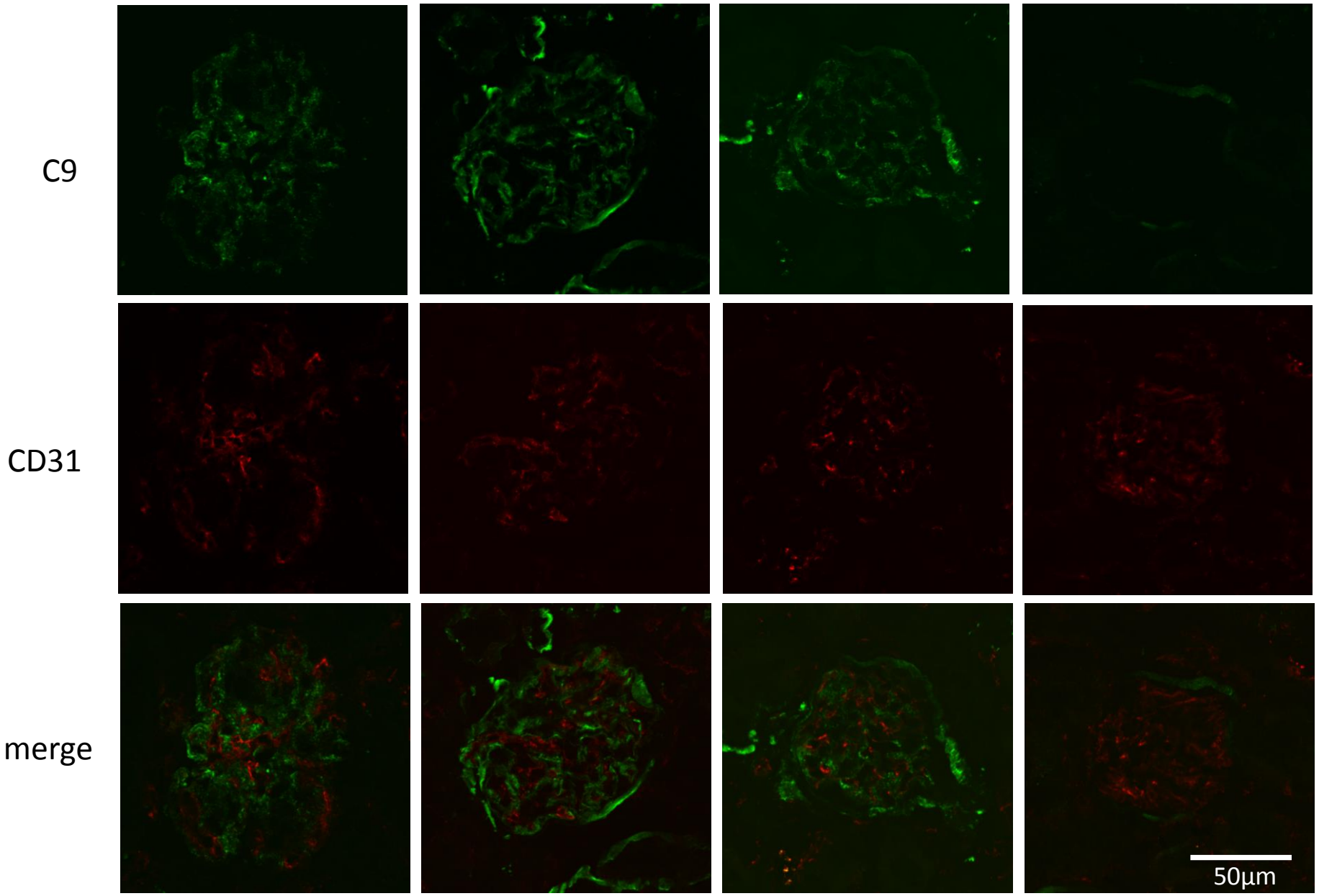

Supplemental Figure 8.

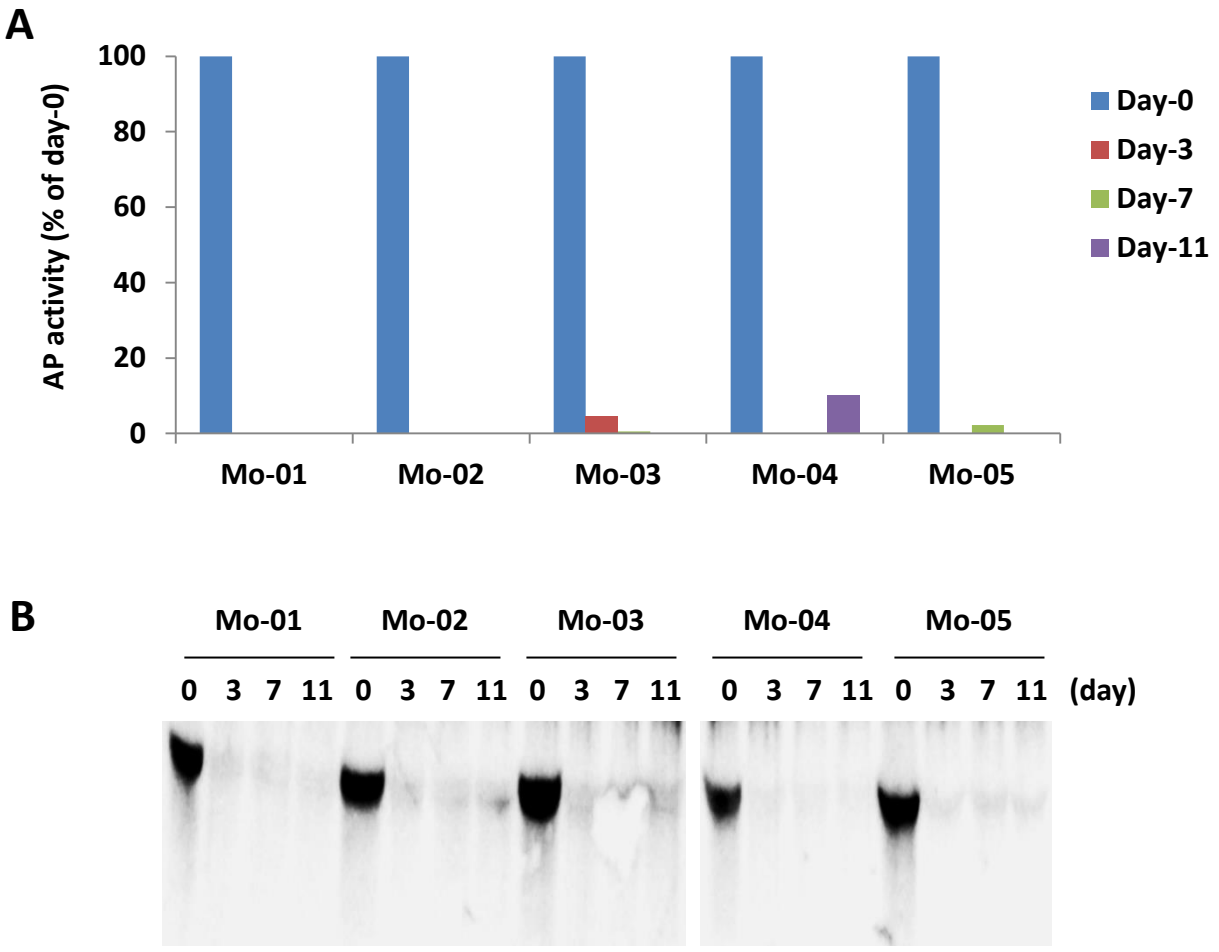

Supplemental Figure 9.

AP activity

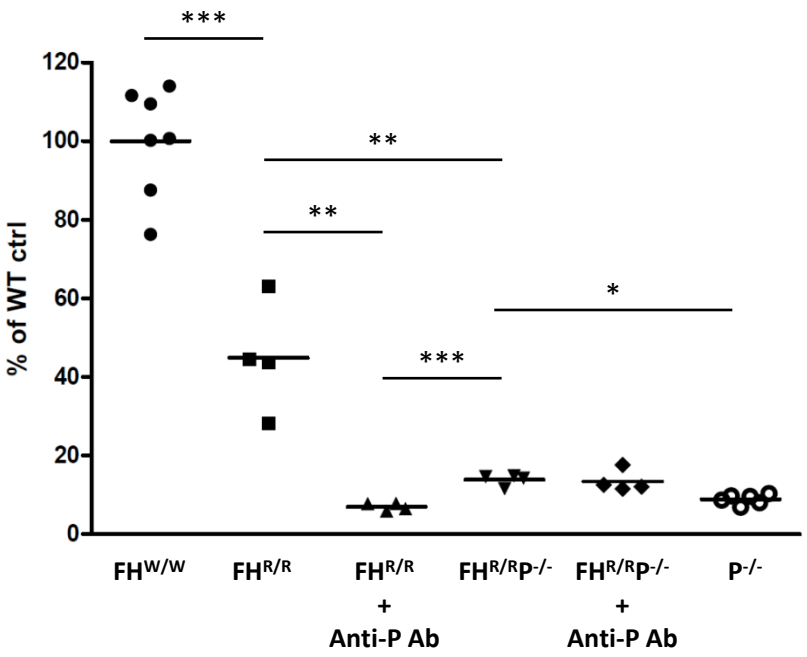

RBC lysis

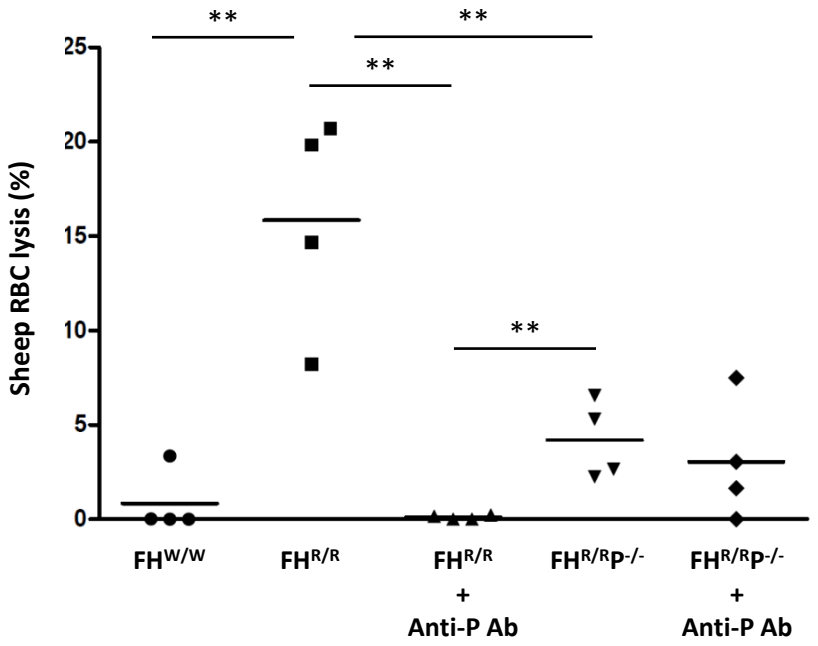

Supplemental Figure 10.

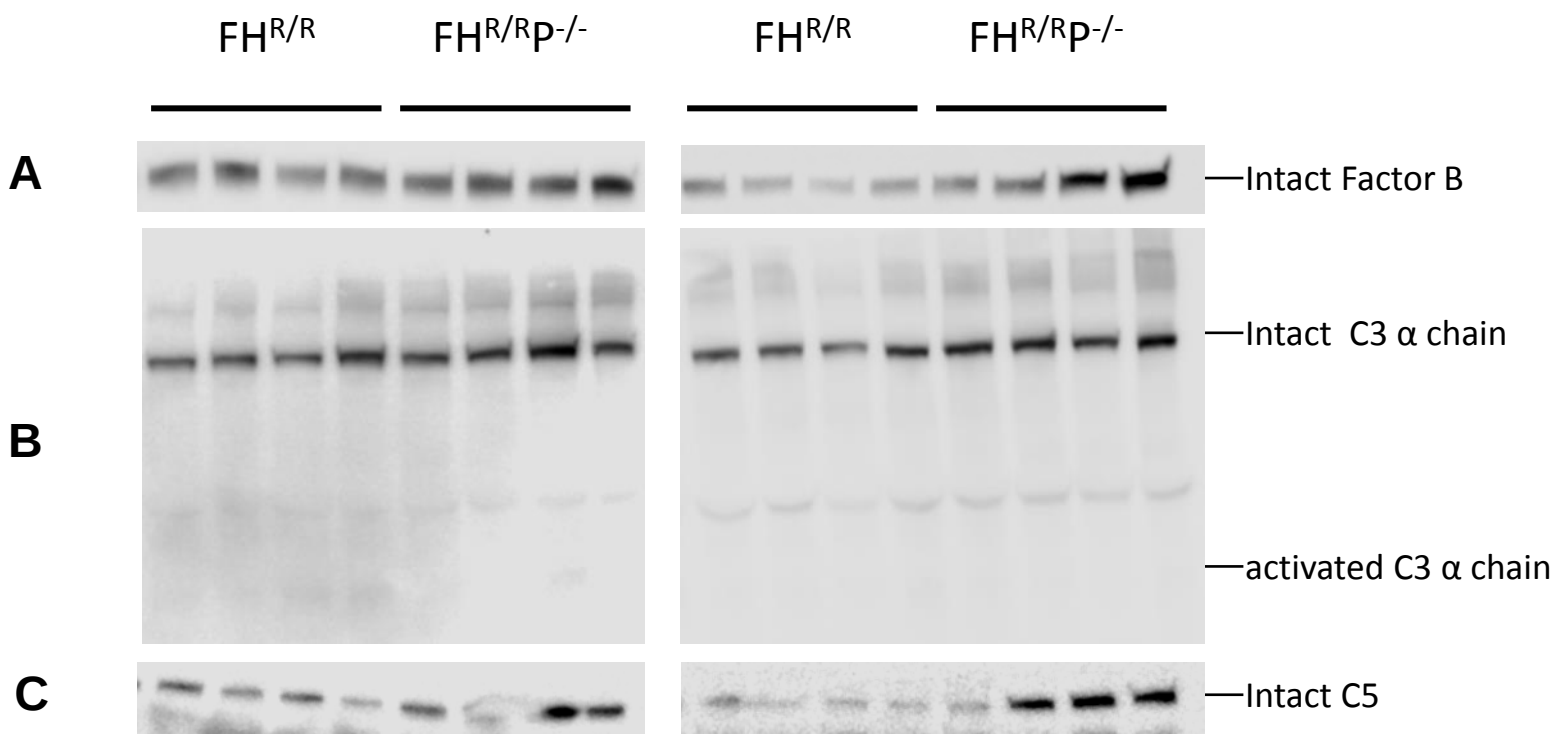

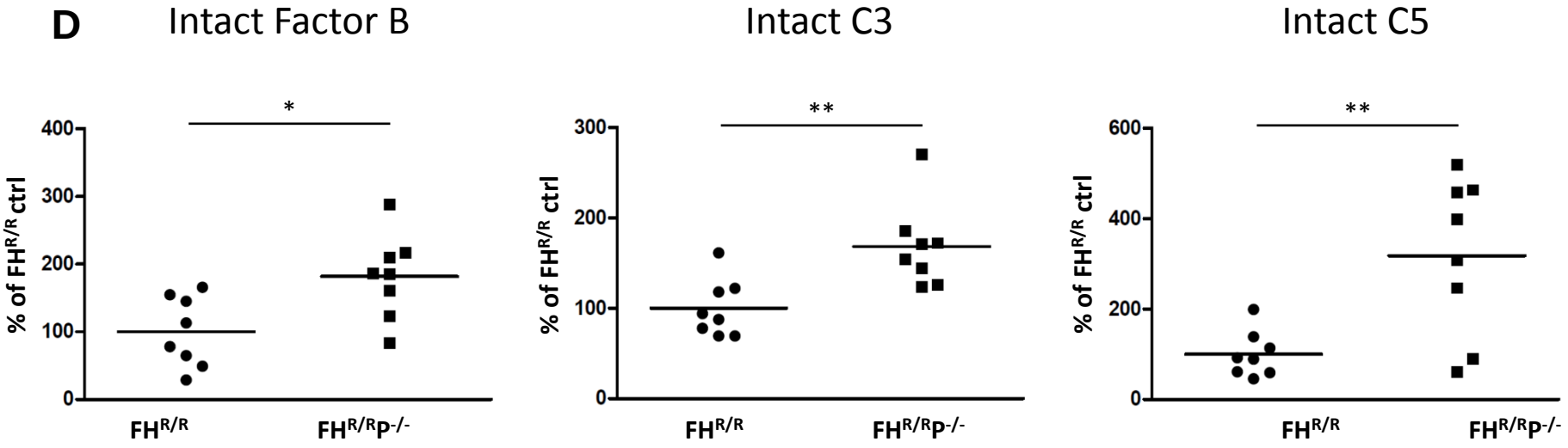

Supplemental Figure 11.

Supplemental Table 1.

Anti-P mAb treatment largely prevented extra-renal phenotypes of $FH^{R/R}$ mice. Serial sections from each organ were prepared and at least 3 non-adjacent sections per tissue sample were examined. To avoid missing the detection of pathological changes, several parts of each organ were harvested and examined. The total number of mice examined, and the number of mice showing a particular pathology (% in brackets) are listed. Neurological abnormality was identified using movement behavior (hemi-paralysis or rapid circular movement) as a surrogate.

Supplemental Figure 1.

Quantitation of glomerular C3 and fibrin fluorescence intensity in $FH^{W/W}$, $FH^{R/R}$, $FH^{R/R}$ $P^{-/-}$ and anti-P mAb-treated $FH^{R/R}$ mice. 10 glomeruli in 3 different viewing fields of each kidney section were evaluated for fluorescence intensity of C3 (A, C) or fibrin (B, D) using ImageJ program and expressed in arbitrary units. Each dot represents the average value from a single mouse. Horizontal bar represents the average value of a group. Mice from each strain were gender mixed and aged 5-20 weeks (A, B) or 14 weeks (C, D). In the anti-P mAb group of panel C and D, 3 mice were treated once-weekly and 3 twice-weekly (n=6 total). *P<0.05, **P<0.01, ***P<0.001 (one-way ANOVA analysis for A and B; Student's t test for C and D).

Supplemental Figure 2.

Glomerular C9 staining in $FH^{W/W}$, $FH^{R/R}$, $FH^{R/R}$ $P^{-/-}$ and anti-P mAb-treated $FH^{R/R}$ mice.

(A) Representative immunofluorescence pictures showing C9 deposition was detected in the glomerulus of $FH^{R/R}$, $FH^{R/R}$ $P^{-/-}$ and anti-P mAb-treated $FH^{R/R}$ but not $FH^{W/W}$ mice. (B) Quantification of immunofluorescence intensity using ImageJ program and expressed in arbitrary units. 10 glomeruli in 3 different viewing fields of each kidney section were evaluated. Each dot represents the average value from a single mouse. Horizontal bar represents the average value of a group. Mice from each strain were gender mixed and aged 5-20 weeks for $FH^{W/W}$, $FH^{R/R}$ and $FH^{R/R}$ $P^{-/-}$ mice and 14 weeks for anti-P mAb-treated $FH^{R/R}$ mice. NS, not significant (Mann-Whitney test).

Supplemental Figure 3.

Glomerular C3 is detected on podocytes of $FH^{R/R}$, $FH^{R/R}$ $P^{-/-}$ and anti-P mAb-treated $FH^{R/R}$ mice. Representative confocal microscopy pictures showing partial co-localization (orange color in merge row) of activated C3 (green) and nephrin (red), a podocyte marker, in the glomeruli of $FH^{R/R}$, $FH^{R/R}$ $P^{-/-}$ and anti-P mAb-treated $FH^{R/R}$ mice. Pictures shown are representative of > 2 kidney sections in each group of mice.

Supplemental Figure 4.

Glomerular C9 is detected on podocytes of $FH^{R/R}$, $FH^{R/R}$ $P^{-/-}$ and anti-P mAb-treated $FH^{R/R}$ mice. Representative confocal microscopy pictures showing partial co-localization (orange color in merge row) of activated C9 (green) and nephrin (red), a podocyte marker, in the glomeruli of $FH^{R/R}$, $FH^{R/R}$ $P^{-/-}$ and anti-P mAb-treated $FH^{R/R}$ mice. Pictures shown are representative of > 2 kidney sections in each group of mice.

Supplemental Figure 5.

Glomerular C3 is detected on mesangium of $FH^{R/R}$, $FH^{R/R}$ $P^{-/-}$ and anti-P mAb-treated $FH^{R/R}$ mice. Representative confocal microscopy pictures showing partial co-localization (orange color in merge row) of activated C3 (green) and platelet-derived growth factor receptor beta (PDGFRb) (red), a mesangial cell marker, in the glomeruli of $FH^{R/R}$, $FH^{R/R}$ $P^{-/-}$ and anti-P mAb-treated $FH^{R/R}$ mice. Pictures shown are representative of > 2 kidney sections in each group of mice.

Supplemental Figure 6.

Glomerular C9 is detected on mesangium of $FH^{R/R}$, $FH^{R/R}$ $P^{-/-}$ and anti-P mAb-treated $FH^{R/R}$ mice. Representative confocal microscopy pictures showing partial co-localization (orange color in merge row) of activated C9 (green) and platelet-derived growth factor receptor beta (PDGFRb) (red), a mesangial cell marker, in the glomeruli of $FH^{R/R}$, $FH^{R/R}$ $P^{-/-}$ and anti-P mAb-treated $FH^{R/R}$ mice. Pictures shown are representative of > 2 kidney sections in each group of mice.

Supplemental Figure 7.

Glomerular C3 is not detected on endothelial cells of $FH^{R/R}$, $FH^{R/R}$ $P^{-/-}$ and anti-P mAb-treated $FH^{R/R}$ mice. Representative confocal microscopy pictures showing no co-localization of activated C3 (green) and CD31 (red), an endothelial cell marker in the glomeruli of $FH^{R/R}$, $FH^{R/R}$ $P^{-/-}$ and anti-P mAb-treated $FH^{R/R}$ mice. Pictures shown are representative of > 2 kidney sections in each group of mice.

Supplemental Figure 8.

Glomerular C9 is not detected on endothelial cells of $FH^{R/R}$, $FH^{R/R}$ $P^{-/-}$ and anti-P mAb-treated $FH^{R/R}$ mice. Representative confocal microscopy pictures showing no co-localization of activated C9 (green) and CD31 (red), an endothelial cell marker in the glomeruli of $FH^{R/R}$, $FH^{R/R}$ $P^{-/-}$ and anti-P mAb-treated $FH^{R/R}$ mice. Pictures shown are representative of > 2 kidney sections in each group of mice.

Supplemental Figure 9

Pharmacodynamics study of properdin inhibition by mAb 14E1 in C57BL/6 mice. (A) C57BL/6 mice (*n*=5) were given a single i.p. injection of 1 mg of mAb 14E1. Plasma samples were collected at the indicated time points and tested for AP activity in LPS-induced AP assay. Injection of 14E1 at 1 mg/mouse resulted in the complete inhibition of AP complement activity for at least 11 days. (B) Western blot analysis of mouse properdin in pre- and post-injection plasma samples showed that mouse properdin was efficiently cleared from the circulation for at least 11 days after 1 mg/mouse mAb 14E1 injection. The clearance of properdin from plasma by mAb 14E1 treatment was consistent with total inhibition of AP complement activity in the treated mice as demonstrated in panel A. Mo-1 to Mo-5 represent individually tested mice.

Supplemental Figure 10

Assessment of AP and lytic complement activities in $FH^{W/W}$, $FH^{R/R}$ and $FH^{R/R}$ $P^{-/-}$ mice. AP complement activity was determined in 10% leprirudin anti-coagulated mouse plasma using LPS-coated ELISA microplate assay and normalized to the average of $FH^{W/W}$ mice. Lytic complement activity was determined in 50% leprirudin anti-coagulated mouse plasma using sheep red blood cell lysis test. Each dot represents a single mouse and horizontal bar through the scattered plots shows the average value of a group. * $p<0.05$, ** $p<0.01$, *** $p<0.001$, Student's t test. In the groups designated as "$FH^{R/R}$ + Anti-P Ab" and "$FH^{R/R}$ $P^{-/-}$ + Anti-P Ab", anti-P mAb was added to the assay plasma *in vitro* (40 μg/ml, final concentration). The data showed that AP and lytic complement activity was markedly reduced in $FH^{R/R}$ $P^{-/-}$ mice compared with $FH^{R/R}$ mice. However, in both assays there was measurable, P-independent activity in $FH^{R/R}$ $P^{-/-}$ mice that could not be blocked by anti-P mAb. Such P-independent activity was not present in $FH^{R/R}$ mice as both AP and lytic activity was completely blocked by anti-P mAb treatment of the plasma. Mice used were of mixed gender and aged 8-16 weeks.

Supplemental Figure 11

Western blot analysis of plasma levels of intact factor B, C3 and C5 in $FH^{R/R}$ and $FH^{R/R}$ $P^{-/-}$ mice. P deficiency reduced consumption and elevated plasma levels of factor B (A, D), C3 (B, D) and C5 (C, D). Eight mice aged 8-16 weeks in each genotype were examined. A-C. Western blot data of 4 representative mice in each group. D. Densitometry scanning of band intensity of 8 mice examined, normalized to the average band signal of $FH^{R/R}$ mice in each Western blot. *p<0.05, **p<0.01, ***p<0.001, Student's t test.